Supplementary Information

Clays and Clay Minerals

Evaluation of the antibacterial properties of commonly used clays from deposits in Central and Southern Asia

Elshan Abdullayev[1,6], Joy R. Paterson[1], M. Daud Hamidi[2], Papreen Nahar[4], H. Chris Greenwell[2,3], Anke Neumann*[5,7], and Gary J. Sharples*[1]

[1]Department of Biosciences, [2]Department of Earth Sciences and [3]Department of Chemistry, Durham University, Stockton Road, Durham, DH1 3LE, UK; [4] Department of Global Health and Infection, Brighton and Sussex Medical School, Sussex University, Brighton, BN1 9PX, UK; [5]School of Engineering, Newcastle University, Newcastle upon Tyne NE1 7RU, UK; [6]Department of Life Sciences, Khazar University, 41 Mehseti Street, Baku, AZ1096, Azerbaijan; [7]Laboratory for Waste Management, Paul Scherrer Institut PSI, Forschungsstrasse 111, 5232 Villigen PSI, Switzerland

Table S1. Elemental composition of aqueous clay leachates determined by ICP-MS.

Source	Afghanistan		Azerbaijan			Bangladesh
Mass / Element	Istalif	Paghman	Bulbula	MGreen	Surakhany	Dhaka
7 / Li	41.11	ND	22.66	73.45	327	23.15
11 / B	529	74.44	328	149	1726	40.91
23 / Na	69810	4535	51967	281600	279700	21083
24 / Mg	24523	6595	5128	30103	48027	14117
27 / Al	**33.45**	**12.44**	**67.50**	**86.28**	**31.14**	**230**
29 / Si	839	1868	1677	1254	158	2090
39 / K	10744	6012	12005	80720	21833	20720
44 / Ca	85757	20580	29427	37177	180767	75493
52 / Cr	0.66	0.95	1.50	1.15	1.26	1.92
55 / Mn	**9.92**	**4.00**	**4.99**	**106**	**138**	**1680**
56 / Fe	**32**	**44.17**	**141**	**58.06**	**ND**	**5008**
59 / Co	ND	ND	ND	ND	ND	29.50
60 / Ni	1.07	0.67	0.74	2.33	5.03	32.91
65 / Cu	4.94	11.14	6.67	13.35	4.64	23.48
66 / Zn	**11.70**	**9.15**	**21.23**	**13.24**	**8.36**	**533**
75 / As	2.22	3.71	3.96	5.03	5.12	4.28
82 / Se	5.06	4.29	6.69	11.56	19.78	4.92
88 / Sr	3562	605	542	996	4747	295
95 / Mo	15.64	7.28	39.56	7.07	8.52	0.29
107 / Ag	ND	ND	ND	ND	ND	ND
111 / Cd	ND	ND	ND	ND	ND	2.89
137 / Ba	17.65	23.06	37.01	14.72	89.33	113
202 / Hg	ND	ND	ND	ND	ND	ND
208 / Pb	1.04	0.80	1.07	59.60	0.59	7.04
238 / U	0.63	0.33	0.46	1.03	1.51	2.30

Element values are provided in parts per billion (ng/ml) and are the average of triplicate analyses. Clay samples (25 mg /ml) were equilibrated for 24 h in deionised water. MGreen, Mashtaga Green; ND, not detected. Toxic metals present at high levels are highlighted in bold.

Table S2. Mineralogy of bulk clays determined by X-ray diffraction.

Source	Afghanistan		Azerbaijan					Bangladesh	
Mineral	Istalif	Paghman	Amircan	Bulbula	MGreen	MYellow	Surakhany	Dhaka	Bhola
Smectite	0	0	0	0	0	0	0	0	0
Illite/Smectite	1.6	TR	11.2	12.1	9.1	15.1	8.2	TR	1.6
Illite+Mica	14.6	17.2	25.5	29.0	34.8	28.8	15.3	32.2	35.4
Kaolinite	0.5	2.0	2.4	3.7	2.3	2.2	1.7	3.6	0.4
Chlorite/Smectite	0	0	0	0	0	0	0	1.2	0
Chlorite	2.0	3.1	4.8	5.3	8.8	4.5	3.3	6.3	4.6
Cristobalite	0	0	0	0	0	0	0	0	0
Quartz	34.2	36.1	34.8	29.2	30.7	30.6	37.3	36.4	40.8
K Feldspar	5.5	4.3	3.1	3.2	2.9	3.0	3.5	6.7	4.9
Plagioclase	22.4	14.0	7.8	9.7	10.2	10.1	11.8	13.5	12.3
Amphibole	2.0	1.3	0	1.1	0	0	0	0	0
Calcite	17.2	19.1	10.3	6.8	0.0	4.9	13.6	0	0
Dolomite	0	2.9	0	0	TR	TR	TR	0	0
Siderite	0	0	0	0	0	0	0	0	0
Halite	0	0	0	0	1.2	0.7	5.3	0	0
Pyrite	0	0	0	0	0	0	0	0	0
Total	100	100	100	100	100	100	100	100	100

The percentage weight determined for each mineral is shown. TR, Trace; MGreen, Mashtaga Green; MYellow, Mashtaga Yellow.

Table S3. Major element composition of bulk clays determined by X-ray fluorescence.

Source	Afghanistan		Azerbaijan					Bangladesh	
Element	Istalif	Paghman	Amircan	Bulbula	MGreen	MYellow	Surakhany	Dhaka	Bhola
Na_2O	1.37	1.35	0.99	1.02	1.98	1.56	2.51	1.10	1.41
MgO	2.57	3.64	2.21	2.37	2.06	2.16	1.75	2.23	2.32
Al_2O_3	15.62	11.98	14.90	17.36	18.96	16.73	12.36	18.66	15.24
SiO_2	52.42	50.72	52.53	53.11	58.19	56.67	52.75	54.90	61.49
P_2O_5	0.09	0.18	0.16	0.14	0.18	0.17	0.16	0.12	0.13
SO_3	<0.01	0.08	0.14	<0.01	<0.01	<0.01	0.05	<0.01	<0.01
K_2O	2.32	2.37	2.58	3.06	3.22	2.90	1.70	3.15	3.24
CaO	6.80	10.39	5.69	3.81	0.45	2.95	8.70	0.92	1.16
TiO_2	0.76	0.65	0.66	0.75	0.86	0.79	0.61	0.79	0.75
Mn_2O_3	0.12	0.12	0.09	0.10	0.08	0.07	0.14	0.07	0.09
Fe_2O_3	6.43	5.16	6.66	6.73	6.10	6.21	4.23	6.21	5.83
BaO	0.07	0.08	0.09	0.08	0.07	0.05	0.26	0.08	0.09
LOI	11.1	12.5	12.5	11.2	7.5	9.3	14.8	11.3	6.7
Total	100	100	100	100	100	100	100	100	100

Percentage values for major elements are shown. MGreen, Mashtaga Green; MYellow, Mashtaga Yellow; LOI, loss on ignition.

Table S4. Minor element composition of bulk clays determined by X-ray fluorescence.

Source	Afghanistan		Azerbaijan					Bangladesh	
Element	Istalif	Paghman	Amircan	Bulbula	MGreen	MYellow	Surakhany	Dhaka	Bhola
V	138	90	128	149	128	144	ND	141	98
Cr	170	103	164	124	106	141	80	126	110
Co	28	21	22	27	22	18	18	24	22
Ni	62	61	64	68	58	54	33	74	50
Cu	39	33	46	40	39	38	21	59	32
Zn	75	81	147	122	97	105	61	143	89
Ga	19	15	22	22	22	20	13	25	20
As	19	12	22	17	16	18	7	10	6
Rb	95	94	99	121	124	114	75	182	166
Sr	278	352	350	223	143	177	386	110	110
Y	26	26	26	28	29	31	25	29	30
Zr	198	186	161	162	185	181	184	150	198
Nb	9	11	11	11	13	14	11	14	14
Sn	2	2	3	3	3	3	2	4	4
Cs	4	4	5	7	8	7	ND	14	9
Ba	396	429	715	507	430	385	1960	560	509
La	32	31	36	36	39	36	21	36	43
Ce	61	63	68	74	73	69	58	78	80
Nd	19	20	23	28	36	31	20	31	36
Hf	4	5	6	ND	6	ND	7	ND	ND
Pb	23	22	90	25	28	24	22	46	25
Th	11	12	10	12	14	13	9	22	19
U	3	3	2	4	3	3	2	8	5

Minor element values are provided in parts per million (ppm). Ge, Se, Mo and Sb were below the limits of detection of 2, 2, 20 and 2 ppm, respectively, as were those labelled ND (not detected). MGreen, Mashtaga Green; MYellow, Mashtaga Yellow.

Table S5. Mineralogy of <2 µm clay fractions determined by X-ray diffraction.

Source	Afghanistan		Azerbaijan					Bangladesh	
Mineral	Istalif	Paghman	Amircan	Bulbula	MGreen	MYellow	Surakhany	Dhaka	Bhola
Smectite	0	0	0	0	0	0	0	0	0
Illite/smectite	27.3	TR	43.7	43.5	29.6	48.7	41.8	TR	36.5
Illite	50.7	68.2	36.5	34.5	41.9	31.8	36.8	63.7	41.7
Kaolinite	9.1	11.6	7.7	7.0	7.4	7.1	7.4	TR	8.4
Chlorite/smectite	0	0	0	0	0	0	0	8.4	0
Chlorite	9.8	14.6	8.8	9.8	14.9	8.3	10.0	24.4	11.0
Quartz	1.7	1.7	3.3	3.6	6.2	4.1	4.0	3.5	2.5
Calcite	1.5	3.9	0	1.6	0	0	0	0	0
Total	100	100	100	100	100	100	100	100	100

The wt.% determined for each mineral is shown. TR, Trace; MGreen, Mashtaga Green; MYellow, Mashtaga Yellow.

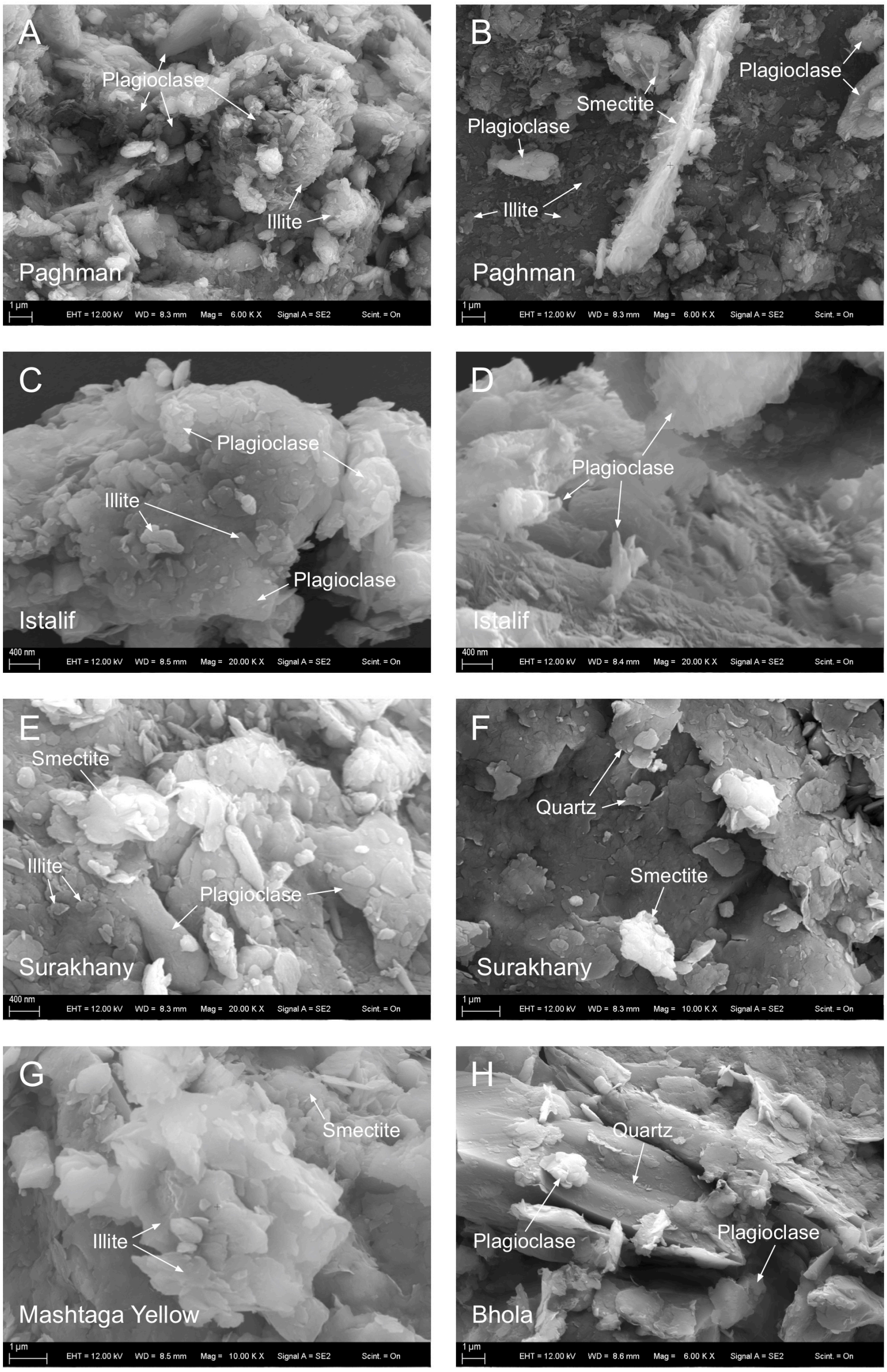

Figure S1. SEM images of minerals present in selected clays. Paghman (A and B) and Istalif (C and D) from Afghanistan, Surakhany (E and F) and Mashtaga Yellow (G) from Azerbaijan and Bhola (H) from Bangladesh. Structures were found with platy morphologies that are distinctive of clay minerals were found (A, B, E, F, and G) and of high aspect ratio crystals with folded edges typical of detrital smectite. Although XRD analysis showed the presence of illite/smectite and mixed-layer chlorite/smectite in the clays, typical hairy shapes or honeycomb structures of mixed-layer clays were not apparent (Abdullayev & Leroy, 2016; Baldermann et al., 2020; Abdullayev et al., 2021). The absence of distinct mixed-layer morphologies in the samples may be due to early-stage transformation of smectite into illite and chlorite, which is supported by the presence of low amounts of illite (10-30%) and chlorite in the respective mixed-layer clays.

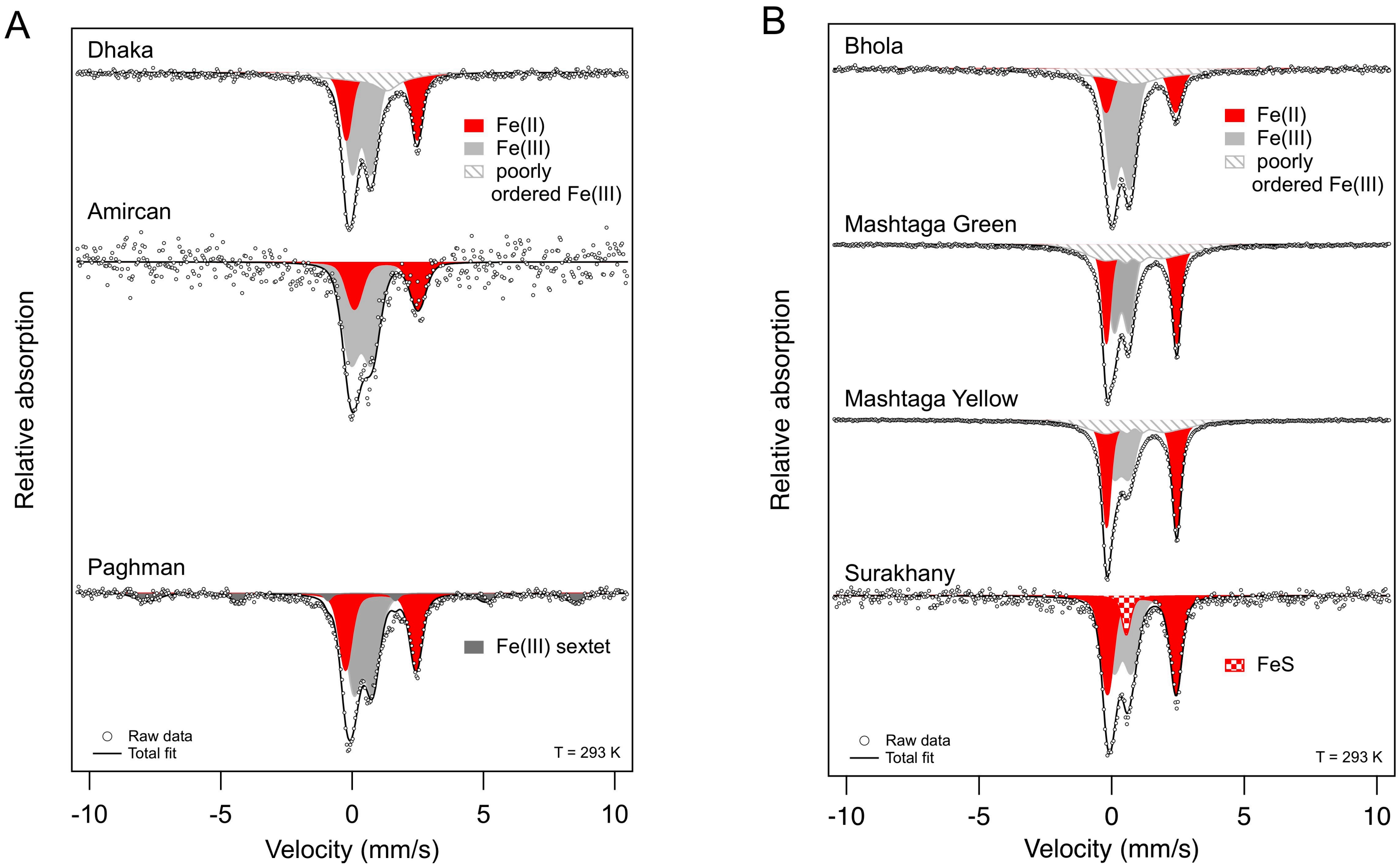

Figure S2. Mössbauer spectra were collected at room temperature (293 K) on selected clay samples (A) displaying antimicrobial activity in suspension and (B) having no effect on the viability of an *E. coli* or *B. subtilis* (compare Fig. 1 C and D). Clay mineral Fe speciation was overall similar across all samples, suggesting that mineral Fe(II) content (red shaded areas) and/or speciation was not responsible for the observed antimicrobial activity or lack thereof.

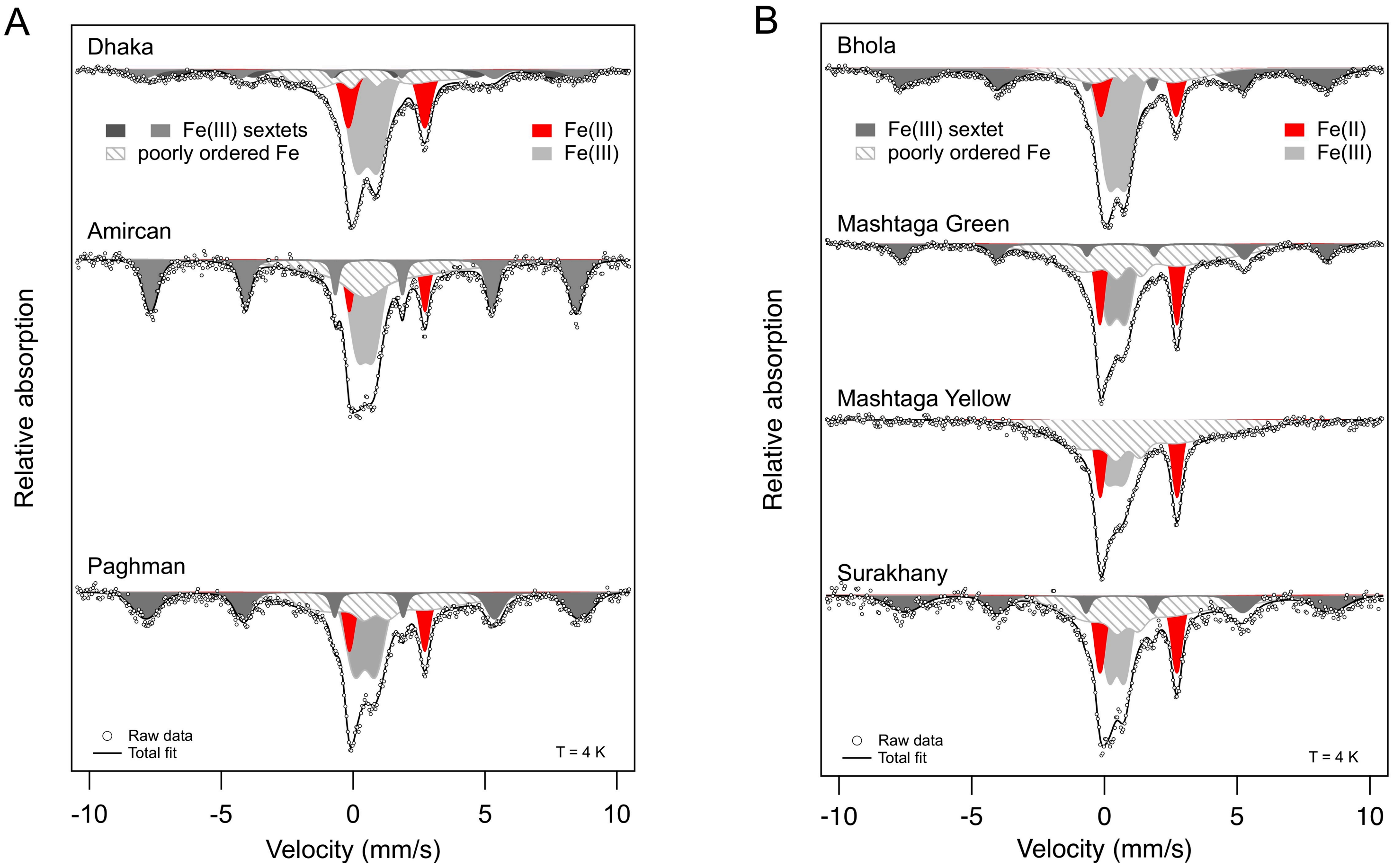

Figure S3. Mössbauer spectra were collected at 4 K on selected clay samples (A) displaying antimicrobial activity in suspension and (B) having no effect on the viability of an *E. coli* or *B. subtilis* (compare Fig. 1 C and D). Clay mineral Fe speciation was overall similar across all samples, suggesting that the extent of magnetic ordering or partitioning into Fe(III) sextets (dark grey areas) and mixed-valent Fe(II)-Fe(III) components (grey striped areas) was not responsible for the observed antimicrobial activity or lack thereof.

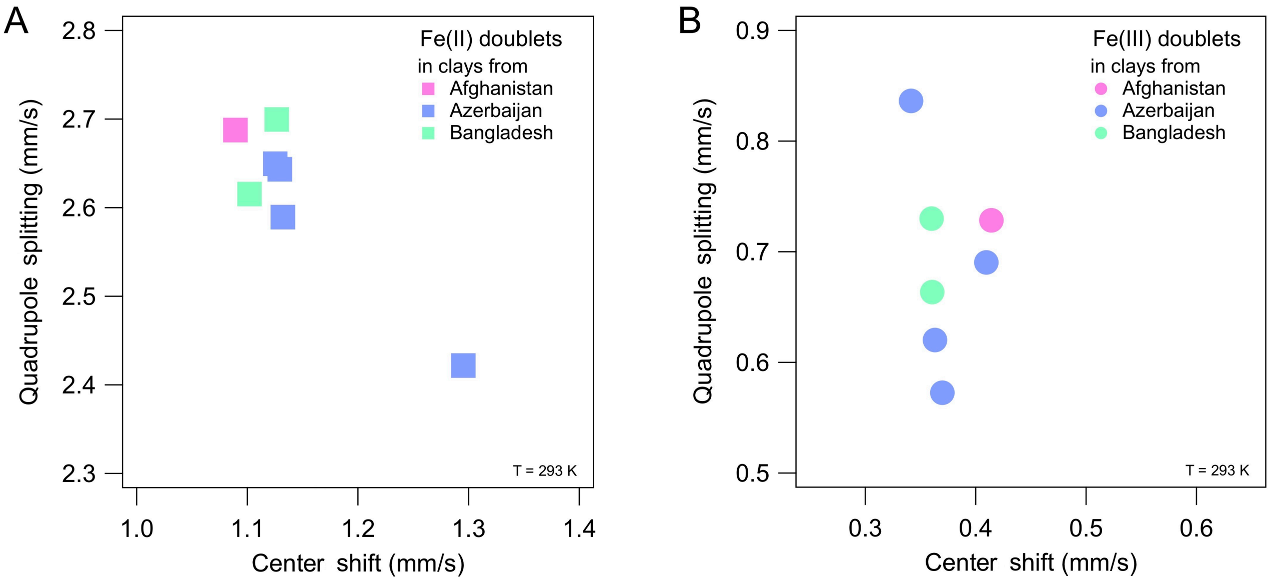

Figure S4. Comparison of hyperfine interaction parameters Center shift (CS) and Quadrupole splitting (QS) for (A) the Fe(II) doublets and (B) the Fe(III) doublets observed in Mössbauer spectra collected at room temperature (293 K) for selected clay mineral samples.

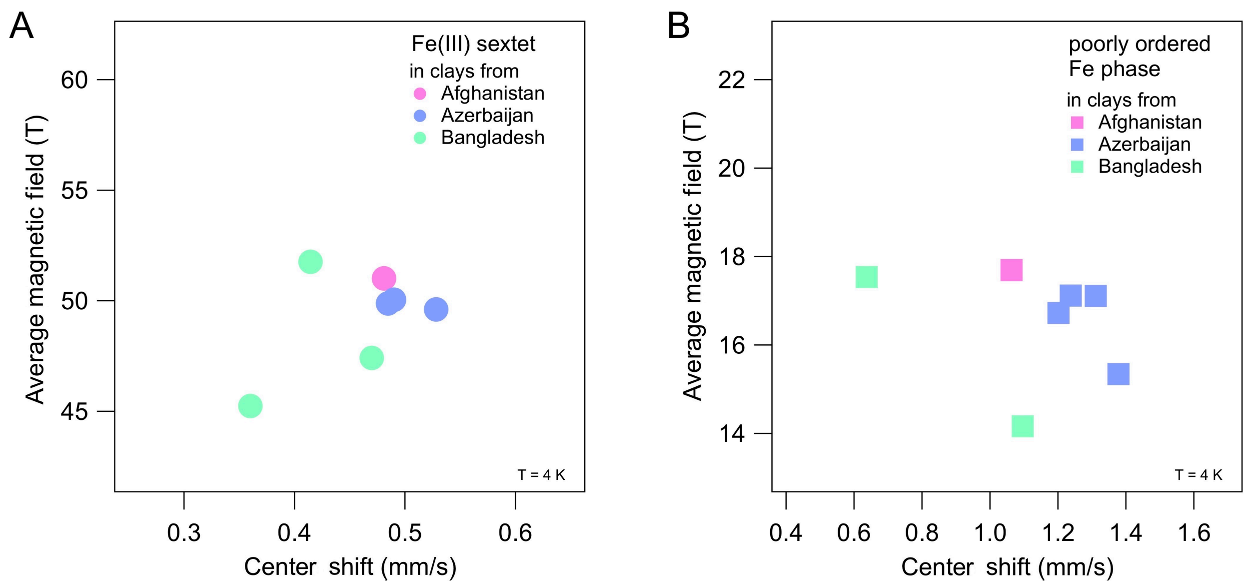

Figure S5. Comparison of hyperfine interaction parameters Center shift (CS) and Magnetic field (H) for (A) the well-ordered Fe(III) sextets and (B) the poorly ordered Fe phases observed in Mössbauer spectra collected at 4 K for selected clay mineral samples. Based on the CS values intermediate between typical Fe(III) and Fe(II) ranges and the low magnetic field value ($H < 18$ T), we assign these poorly ordered features to mixed-valent Fe(II)-Fe(III)-containing phases.

Table S6. Mössbauer hyperfine parameters of selected clay samples from Afghanistan (Paghman), Azerbaijan (Amircan, Mashtaga Green and Yellow, Surakhany) and Bangladesh (Dhaka, Bhola). Spectra were acquired at room temperature (293 K) and at 4 K and were evaluated for Mössbauer parameters using a Voigt-based fitting routine (Rancourt & Ping, 1991).

		293 K					4 K				
Sample	**Component**	**<CS>**[b]	**<|QS|> or <ε>**[c]	**<|H|>**[d]	**σ(|H| or |QS|)**[e]	**Area (σ)**[f]	**<CS>**[b]	**<|QS|> or <ε>**[c]	**<|H|>**[d]	**σ(|H| or |QS|)**[e]	**Area (σ)**[f]
(χ^2)[a]		mm/s	mm/s	T	T or mm/s	%	mm/s	mm/s	T	T or mm/s	%
Paghman (1.80/0.67)	Fe(II)	1.09	2.69		0.36	36.6 (0.8)	1.29	2.86		0.26	13.4 (1.2)
	Fe(III)	0.41	0.73		0.40	49.8 (0.9)	0.46	0.84		0.50	28.0 (2.7)
	Fe(III) sextet	0.34	-0.02	50.4	2.4	13.6 (1.1)	0.53	-0.11	51.0	2.8	27.5 (2.0)
	poorly ordered Fe(III)						1.06	0.20	17.7	9.6	31.1 (3.2)
Amircan (0.60/0.62)	Fe(II)	1.30	2.42		0.49	31.8 (5.2)	1.29	2.87		0.19	9.8 (1.2)
	Fe(III)	0.34	0.84		0.49	68.2 (5.2)	0.47	0.68		0.43	27.6 (1.9)
	Fe(III) sextet						0.49	-0.10	50.0	1.4	32.0 (1.9)
	poorly ordered Fe(III)						1.20	0.77	16.7	12.6	30.6 (2.8)
Mashtaga Green (1.61/0.80)	Fe(II)	1.13	2.65		0.2	37.1 (0.6)	1.28	2.90		0.2	19.4 (0.7)
	Fe(III)	0.37	0.57		0.3	37.4 (0.7)	0.47	0.70		0.4	25.6 (1.2)
	Fe(III) sextet						0.48	-0.12	49.9	1.9	13.6 (0.8)
	poorly ordered Fe(III)	0.92	0.12	10.2	4.7	25.5 (0.7)	1.24	0.31	17.1	8.2	41.4 (1.3)
Mashtaga Yellow (2.39/0.71)	Fe(II)	1.13	2.64		0.19	37.1 (0.6)	1.29	2.89		0.25	22.1 (1.3)
	Fe(III)	0.36	0.62		0.37	37.4 (0.7)	0.41	0.75		0.48	25.1 (2.2)
	poorly ordered Fe(III)	0.92	0.06	10.3	4.0	25.5 (0.7)	1.31	0.42	17.1	8.9	52.8 (2.3)
Surakhany (0.72/0.67)	Fe(II)	1.13	2.59		0.33	50.5 (5.5)	1.28	2.89		0.27	18.7 (1.8)
	Fe(III)	0.41	0.69		0.38	41.5 (5.5)	0.46	0.61		0.35	23.1 (3.0)
	Fe(III) sextet						0.53	-0.04	49.6	3.5	21.6 (2.4)
	poorly ordered Fe(III)						1.38	0.49	15.3	8.4	36.6 (3.6)
	FeS	0.55	0.16		0.1	8.0 (6.5)					
Dhaka (0.75/0.94)	Fe(II)	1.13	2.70		0.30	31.3 (1.3)	1.26	2.90		0.37	17.9 (0.5)
	Fe(III)	0.36	0.73		0.37	51.4 (1.8)	0.54	0.86		0.53	38.9 (0.8)
	Fe(III) sextet 1						0.36	-0.07	45.2	3.4	10.0 (0.9)
	Fe(III) sextet 2						0.41	-0.10	51.8	2.8	10.1 (0.9)
	poorly ordered Fe(III)	0.52	-0.81	8.3	6.3	17.2 (2.2)	0.64	0.23	17.5	6.6	23.1 (0.9)
Bhola (0.87/0.88)	Fe(II)	1.10	2.62		0.35	20.9 (0.8)	1.28	2.83		0.31	12.9 (0.8)
	Fe(III)	0.36	0.66		0.35	55.4 (1.5)	0.48	0.73		0.45	38.9 (1.0)
	Fe(III) sextet						0.47	-0.11	47.7	5.4	32.5 (1.1)
	poorly ordered Fe(III)	0.55	-0.33	17.1	12.9	23.7 (1.8)	1.10	0.02	14.2	4.8	15.7 (1.3)

[a]Reduced chi-squared value for the fit of the data collected at 293 K / collected at 4 K. [b]Centre shift relative to α-Fe(0). [c]Average quadrupole split value of a doublet (QS) or average quadrupole shift value of a sextet (ε). [d]Average magnetic field of the hyperfine field magnetic distribution (sextet). [e]Standard deviation width of the QS or H distribution. [f]Standard deviation due to uncertainty.

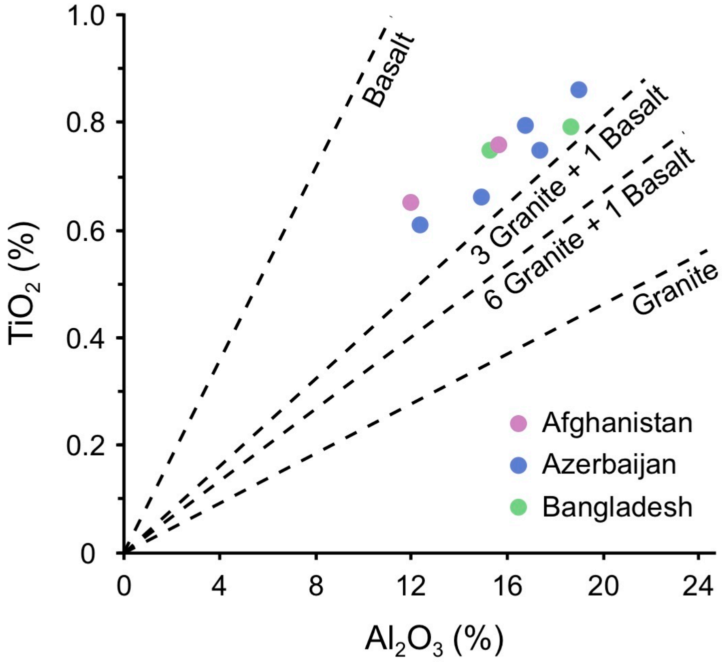

Figure S6. TiO_2 versus Al_2O_3 plot for Afghanistan, Azerbaijan and Bangladesh clays.

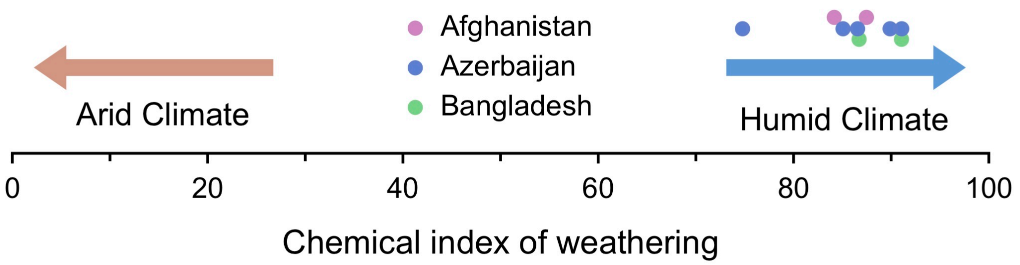

Figure S7. Chemical index of weathering (CIW) in Afghanistan, Azerbaijan and Bangladesh clays.

References

Abdullayev, E. & Leroy, S.A.G. (2016) Provenance of clay minerals in the sediments from the Pliocene Productive Series, western South Caspian Basin. *Mar. Pet. Geol.*, **73**, 517-527.

Abdullayev, E., Baldermann, A., Warr, L.N., Grathoff, G. & Taghiyeva, Y. (2021) New constraints on the palaeo-environmental conditions of the Eastern Paratethys: implications from the Miocene Diatom Suite (Azerbaijan). *Sediment. Geol.*, **411**, 105794.

Baldermann, A., Abdullayev, E., Taghiyeva, Y., Alasgarov, A. & Javad-Zada, Z. (2020) Sediment petrography, mineralogy and geochemistry of the Miocene Islam Dağ Section (Eastern Azerbaijan): Implications for the evolution of sediment provenance, palaeo-environment and (post-)depositional alteration patterns. *Sedimentology*, **67**, 152-172.

Rancourt, D.G. & Ping, J.Y. (1991) Voigt-based method for arbitrary-shape static hyperfine parameter distributions on Mössbauer-spectroscopy. *Nuclear Instruments & Methods in Physics Research Section B-Beam Interactions with Materials and Atoms*, **58**, 85-97.